Buckling Analysis of FG Plate with Smart Sensor/Actuator

N.S. Viliani[1,*], S.M.R. Khalili[2,3], H. Porrostami[1]

[1]*Department of Mechanical Engineering, Islamic Azad University, Abhar Branch, Abhar, Iran*
[2]*Faculty of Mechanical Engineering, K.N. Toosi University of Technology, Tehran, Iran*
3*Faculty of Engineering, Kingston University, London, UK*

ABSTRACT

In this paper, the active buckling control of smart functionally graded (FG) plates using piezoelectric sensor/actuator patches is studied. A simply supported FG rectangular plate which is bonded with piezoelectric rectangular patches on the top and/or the bottom surface(s) as actuators/sensors is considered. When a constant electric charge is imposed, the governing differential equations of motion are derived using the classical laminated plate theory (CLPT). The solution for the equation of motion is obtained using a Fourier series method and the effect of feedback gain on the critical buckling load for PZT-4 is studied .The buckling behavior of smart plate subjected to compressive load is also investigated. The sensor output is used to determine the input to the actuator using the feedback control algorithm. The forces induced by the piezoelectric actuators under the applied voltage field, enhance the critical buckling load.

© 2009 IAU, Arak Branch. All rights reserved.

Keywords: Smart functionally graded materials; Piezoelectric; Buckling; Sensor; Actuator

1 INTRODUCTION

THE coupling of the elastic and electric fields in piezoelectric materials is used in smart plates and shells by bonding piezoelectric patches for sensing and control. A foundation work on the buckling of structures is presented by Brush and Almoroth [1]. They examined the effect of initial imperfection on the critical loads. Turvey and Marshall [2] studied the buckling and postbuckling of composite plates due to the mechanical and thermal loads. Many investigations are conducted on the stability analysis of imperfect structures. Elastic, plastic and creep buckling of imperfect cylinders under mechanical and thermal loads is studied by Eslami and Shariyat [3]. Mossavarali and Eslami [4] studied the thermoelastic buckling of isotropic and orthotropic plates with imperfection. Murphy and Ferreira [5] investigated thermal buckling analysis of clamped rectangular plates based on energy consideration. The first application of piezoelectric material is referred to the experimental work of Bailey and Hubbard [6], in which this material was used as actuators for the vibration control. Recently, several attempts are made to overcome these problems by using Functionally Graded Materials (FGMs) [7]. FGMs are novel and microscopically inhomogeneous in which the mechanical properties vary smoothly and continuously from one surface to another. It has many favorable performances in engineering application such as high resistance to large temperature gradient and reduction of stress concentration. Comprehensive works on the post-buckling of structures of purely FGM or FG laminated plates have been reported in the literatures. Feldman and Aboudi [8] studied the elastic bifurcation buckling of FG plate under in-plane compressive load and presented the buckling loads of rectangular plates with both simply supported and clamped edges. Woo and Meguid [9] derived an analytical solution expressed in terms of Fourier series for large displacement of FG plates and shallow shells under both transverse mechanical loading and temperature rise fields. Javaheri and Eslami [10] investigated the thermal buckling of rectangular FG plate based on classical as well as higher-order shear deformation theories and obtained

---

* Corresponding author. Tel: +98 21 2237 8012 and 0916 313 8696.
  E-mail address: vnavid@hotmail.com.

the closed form solution of the problem under several types of thermal loadings. From the various kinds of materials available for use in the smart structures, only piezoelectrics have the unique capability to be used effectively as both actuator and sensor elements. Still various different piezoelectric materials like PZT-2, PZT-4, PZT-5, PVDF and PMN are under investigation for aerospace and other applications. Moreover, since the PZT has higher piezoelectric, dielectric and elasticity coefficients it is widely used in different industrial applications.

The fundamental work of Tiersten [11] gave much of the necessary theoretical development for the static and dynamic behavior of a single-layer piezoelectric plate. Lee and Moon [12], and Lee [13] used the assumption of Classical Laminated Plate Theory (CLPT) to derive a simple model for analysis of piezoelectric laminates, used primarily in designing the piezoelectric laminates in bending and torsional control. In the work of Thompson and Loughlan [14], the active buckling control is examined using an analytical model and experimental procedure. In the work of Varelis and Saravanos [15], the initial buckling of smart beams and plates is studied using an electromechanically coupled formulation in combination with an 8-node FE and the critical buckling load is examined by altering the electrical conditions. The issue of active buckling compensation is also tackled for smart plates, however, the thermal effects are not incorporated. More recently, Yang [16] included higher order (quadratic) electric potential variation through the thickness of the actuators and obtained a two-dimensional equation for bending motion of an elastic plate with partially electroded piezoelectric actuators attached to the top and the bottom surfaces of a thick plate. Due to the added weight effect and the difficulties in the fabrication considerations instead of covering the entire surface in the form of layers, a discrete monolithic type of piezoelectric material can also be used for sensing and control purposes. In other words, when a single piece of fully distributed piezoelectric sensor-actuator is used, there are some observability and controllability deficiencies in monitoring and controlling the plate and the shell responses [17]. Spatial shaping of distributed sensor and actuator, for example by segmenting them into a number of smaller pieces, can improve the controllability and observability. The effectiveness of distributed piezoelectric sensor and actuators in the form of rectangular patch, bonded on simply supported rectangular thin composite plates and circular cylindrical shell have been investigated by Tzou and Fu [18]. Kargarnovin et al. [19] investigated the vibration control of a FG plate patched with piezoelectric actuators and sensors under a constant electric charge.

In this paper, the active buckling of smart FG plates using piezoelectric sensor/actuator patches is studied. The plate is simply supported and is bonded with piezoelectric rectangular patches on the top and/or the bottom surfaces as actuators or sensors. The classical plate theory is used to derive the governing differential equations of motion. The solution is obtained by Fourier series and the effect of feedback of FG plate on the critical buckling load for PZT-4 piezoelectric patches is studied. The sensor output is used to determine the input to the actuator using the feedback control algorithm.

2   MATHEMATICAL FORMULATION AND MATERIAL DESCRIPTION
2.1 Strain-displacement relations

The displacement field is based on classical laminated composite plate theory and is expressed as follows [20]

$$u(x,y,z,t) = u_0(x,y,t) - z \frac{\partial w_0}{\partial x} \tag{1}$$

$$v(x,y,z,t) = v_0(x,y,t) - z \frac{\partial w_0}{\partial y} \tag{2}$$

$$w(x,y,z,t) = w_0(x,y,t) \tag{3}$$

where u_0, v_0, w_0 are the displacements along the x, y, z coordinate directions, respectively for a point on the mid-plane ($z = 0$). Assuming the small displacements, the strain-displacement relations take the form

$$\begin{Bmatrix} \varepsilon_{xx} \\ \varepsilon_{yy} \\ \varepsilon_{xy} \end{Bmatrix} = \begin{Bmatrix} \varepsilon_{xx}^0 \\ \varepsilon_{yy}^0 \\ \varepsilon_{xy}^0 \end{Bmatrix} + z \begin{Bmatrix} k_x \\ k_y \\ k_{xy} \end{Bmatrix} \tag{4}$$

where

$$(\varepsilon_{xx}^0 \quad \varepsilon_{yy}^0 \quad \varepsilon_{xy}^0)^T = \left(\frac{\partial u_0}{\partial x} \quad \frac{\partial v_0}{\partial y} \quad \frac{\partial u_0}{\partial y} + \frac{\partial v_0}{\partial x} \right)^T \tag{4a}$$

$$(k_x \quad k_y \quad k_{xy})^T = \left(-\frac{\partial^2 w_0}{\partial x^2} \quad -\frac{\partial^2 w_0}{\partial y^2} \quad -2\frac{\partial^2 w_0}{\partial x \, \partial y} \right)^T \tag{4b}$$

2.2 FG plates

FGMs are microscopically inhomogeneous materials with the mechanical properties vary smoothly and continuously through the thickness. FGMs are typically made from a mixture of ceramics and metals or a combination of different metals. The ceramic constituent of the material provides the temperature resistance due to its low conductivity and the metal parts prevents fracture caused by stresses due to high temperature gradient in very short period of time [21]. Furthermore, a mixture of a ceramic and a metal with a continuously varying volume fraction can be easily manufactured. The coordinate system and definition of the FG plate with piezoelectric patches are shown in Fig. 1. In this work, it is possible to consider the FGM properties, E, varies according to the following expressions [22]

$$E = E(z) = E_1 e^{\beta z} \tag{6a}$$

$$\upsilon_{FGM} = \text{const.} \tag{6b}$$

where

$$\beta = \frac{1}{b} \ln \left(\frac{E_2}{E_1} \right) \tag{7}$$

where E_1 and E_2 are the value of elastic modulus at $x=0$ and $x=b$, respectively, where b is the width of the FG plate. The Poisson's ratio υ, is considered to be constant.

2.3. Stress–strain relation in FG plate

The stress-strain relations for the FG plate are similar to those of orthotropic plates. The only difference is related to the elasticity modules which is no longer constant. Hence, the constitutive relations for the FG laminate are [21]
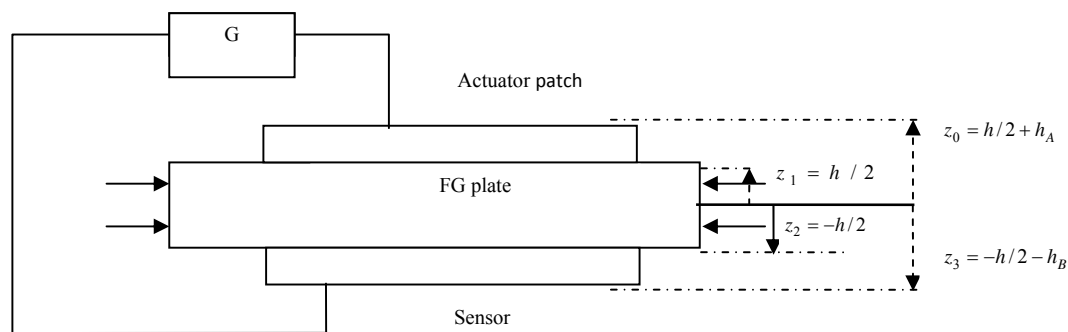

Fig. 1
Coordinate system and definitions of FG plate with piezoelectric patches as sensor and actuator fixed to the lower and upper sides along with the controlling circuit.

$$\begin{Bmatrix} \sigma_{xx} \\ \sigma_{yy} \\ \tau_{yz} \\ \tau_{xz} \\ \tau_{xy} \end{Bmatrix} = \begin{bmatrix} c_{11} & c_{12} & 0 & 0 & 0 \\ c_{21} & c_{22} & 0 & 0 & 0 \\ 0 & 0 & c_{44} & 0 & 0 \\ 0 & 0 & 0 & c_{55} & 0 \\ 0 & 0 & 0 & 0 & c_{66} \end{bmatrix} \begin{Bmatrix} \varepsilon_{xx} \\ \varepsilon_{yy} \\ \varepsilon_{yz} \\ \varepsilon_{xz} \\ \varepsilon_{xy} \end{Bmatrix} \tag{8}$$

in which $c_{11} = c_{22} = \dfrac{E(z)}{1 - \upsilon_{fgm}^2}$, $\quad c_{21} = c_{12} = \upsilon_{fgm} c_{11}$, $\quad c_{44} = c_{55} = c_{66} = \dfrac{E(z)}{2(1 + \upsilon_{fgm})}$ and σ_{ii} are the normal stresses , τ_{ij} are the shear stresses and ε_{ij} are the corresponding strains.

2.4 Piezoelectric materials stress–strain relations

The constitutive relations in terms of non-zero stress and strain components for the attached piezoelectric patches are [23]

$$\{\sigma\} = [C]\{\varepsilon\} - [e]^T\{E\} \tag{9a}$$
$$\{D\} = [e]\{E\} + [\in]\{E\} \tag{9b}$$

or in the matrix forms as

$$\begin{Bmatrix} \sigma_{xx} \\ \sigma_{yy} \\ \tau_{xy} \end{Bmatrix} = \begin{bmatrix} c_{11} & c_{12} & 0 \\ c_{21} & c_{22} & 0 \\ 0 & 0 & c_{66} \end{bmatrix} \begin{Bmatrix} \varepsilon_{xx} \\ \varepsilon_{yy} \\ \varepsilon_{xy} \end{Bmatrix} - \begin{bmatrix} 0 & 0 & e_{13} \\ 0 & 0 & e_{23} \\ 0 & 0 & 0 \end{bmatrix} \begin{bmatrix} E_x \\ E_y \\ E_z \end{bmatrix} \tag{10a}$$

$$\begin{Bmatrix} D_x \\ D_y \\ D_Z \end{Bmatrix} = \begin{bmatrix} 0 & 0 & 0 \\ 0 & 0 & 0 \\ e_{31} & e_{32} & 0 \end{bmatrix} \begin{Bmatrix} \varepsilon_{xx} \\ \varepsilon_{yy} \\ \varepsilon_{xy} \end{Bmatrix} + \begin{bmatrix} \in_{11} & 0 & 0 \\ 0 & \in_{22} & 0 \\ 0 & 0 & \in_{33} \end{bmatrix} \begin{bmatrix} E_x \\ E_y \\ E_z \end{bmatrix} \tag{10b}$$

in which $\{\sigma\}$ represents the column of stress components, $\{\varepsilon\}$ the column of strain components, $\{E\}$ the column of electrical field components, $\{D\}$ the column of the electrical displacement components, [C] the matrix of elastic constants, $[e]$ the piezoelectric stress coefficient matrix and $[\in]$ the dielectric permittivity matrix in which

$$[e] = [d][C] \tag{11}$$

where [d] is the piezoelectric strain coefficient matrix.

2.5 Actuator and sensor's constitutive relations
2.5.1 Actuator's constitutive relation

For a piezoelectric actuator patch the Maxwell's equations are [25]

$$D = \in .E \qquad \Rightarrow \qquad \nabla.D = 0 \tag{12}$$

in which D, $\in$, and E are electric displacement, dielectric constant and electric field, respectively. If the patch is thin, then it can be assumed that x and y components of the electric displacement field are constant within the patch along x and y directions, hence the charge Eq. (12) reduces to [24]

$$\frac{\partial D_x}{\partial x} + \frac{\partial D_y}{\partial y} + \frac{\partial D_z}{\partial z} = 0 \rightarrow \frac{dD_z}{dz} = 0 \tag{13}$$

Moreover, it is assumed that the electric potential inside the actuator patch varies quadratically in the *z*-direction, i.e.

$$\phi^a = \phi_0 + z\phi_1 + z^2\phi_2 \tag{14}$$

Furthermore, it is assumed that the electric boundary conditions for the actuator patch are

$$\phi = V^a \quad at \quad z = z_0 = \frac{h}{2} + h_A$$
$$\phi = 0 \quad at \quad z = z_1 = \frac{h}{2} \tag{15}$$

Using these conditions in Eq. (14) yields to

$$\phi_1^a = \frac{V^a}{h_A} - (h_A + h)\phi_2^a \tag{16}$$

in which, $h_A = (z_0 - z_1)$ is thickness of actuator. Now by combining Eq. (10b) and (13) and considering $E_z = -\dfrac{\partial \phi}{\partial z}$, it can be obtained

$$\phi_2^a = -\frac{e_{13}}{2 \in_{33}}\left(\frac{\partial^2 w}{\partial x^2} + \frac{\partial^2 w}{\partial y^2}\right) \tag{17}$$

By substituting Eqs. (16) and (17) into Eq.(14) , the electric field inside the actuator patch becomes

$$E_z = -\frac{\partial \varphi}{\partial z} = -\frac{V^a}{h_A} + e_{13}\left(\frac{h_m^a - z}{\in_{33}}\right)\left(\frac{\partial^2 w}{\partial x^2} + \frac{\partial^2 w}{\partial y^2}\right)^a \tag{18}$$

in which, $h_m^a = \left(\dfrac{z + z_0}{2}\right) = \left(\dfrac{h + h_A}{2}\right)$. In the next step by substituting Eq. (18) into Eq. (10a), the stress- strain relation for the actuator patch yields to

$$\sigma_{xx}^a = c_{11}^a\varepsilon_{xx}^a + c_{12}^a\varepsilon_{yy}^a + \frac{e_{31}V^a}{h_A} - \frac{e_{31}^2(z - h_m^a)}{\in_{33}}\left(\frac{\partial^2 w}{\partial x^2} + \frac{\partial^2 w}{\partial y^2}\right)$$

$$\sigma_{yy}^a = c_{12}^a\varepsilon_{xx}^a + c_{22}^a\varepsilon_{yy}^a + \frac{e_{31}V^a}{h_A} - \frac{e_{31}^2(z - h_m^a)}{\in_{33}}\left(\frac{\partial^2 w}{\partial x^2} + \frac{\partial^2 w}{\partial y^2}\right) \tag{19}$$

$$\tau_{xy} = c_{66}\gamma_{xy}$$

2.5.2. Sensor constitutive relation

From the reduced charge equation, the *z* component of the electric displacement of the sensor patch should be constant along the thickness (*z*-direction, see Eq. (14)). On the other hand, since there is no external supply of

electric charge to the patch, the total charge which appears on the sensor patch electrode surfaces should be zero. This condition can be represented as $D_z \mid_{z=z_1} + D_z \mid_{z=z_2} = 0$. From this condition and the reduced charge equation which is zero i.e. $D_z = 0$, everywhere inside the patch, it is possible to get

$$D_z = e_{13}\varepsilon_{xx} + e_{13}\varepsilon_{yy} + \in_{33} E_z^s \tag{20}$$

Then, the electric field in the sensor can be obtained as

$$E_z^s = -\frac{e_{31}}{\in_{33}}\left\{\left(\frac{\partial u_0}{\partial x} + \frac{\partial v_0}{\partial y}\right) - z\left(\frac{\partial^2 w}{\partial x^2} + \frac{\partial^2 w}{\partial y^2}\right)\right\}^s \tag{21}$$

Now by substitution Eq. (21) into constitutive Eq. (10a), the stress-strain relation for the sensor patch can be obtained as

$$\sigma_{yy}^s = \left(c_{21} + \frac{e_{31}^2}{\in_{33}}\right)\varepsilon_{xx}^s + \left(c_{22} + \frac{e_{31}^2}{\in_{33}}\right)\varepsilon_{yy}^s$$

$$\sigma_{xx}^s = \left(c_{11} + \frac{e_{31}^2}{\in_{33}}\right)\varepsilon_{xx}^s + \left(c_{12} + \frac{e_{31}^2}{\in_{33}}\right)\varepsilon_{yy}^s \tag{22}$$

$$\tau_{xy}^s = c_{66} y_{xy}^s$$

The average sensor potential (the voltage that appears between sensor electrodes) is

$$V^s = \frac{1}{A_s}\int\left(\phi^s \mid_{z=z_2} - \phi^s \mid_{z=z_3}\right) dA = \frac{h_s e_{31}}{A_s \in_{33}}\left\{\int\left(\frac{\partial u_0}{\partial x} + \frac{\partial v_0}{\partial y}\right) + \left(\frac{h+h_s}{2}\right)\left(\frac{\partial^2 w}{\partial x^2} + \frac{\partial^2 w}{\partial y^2}\right) dA\right\} \tag{23}$$

When the structure oscillates, a real-time voltage (V^a) signal will be generated in the sensor. The signal is fed to the control algorithm that determines the power input of the distributed actuator on the top plate as shown in Fig. 1. If V^a is the actuating voltage as determined by the control algorithm, and the sensor signal is V^s for the constant gain control algorithm, then, V^a is obtained by the following

$$V^a = GV^s, \qquad V^a = -\frac{e_{31}Gh_s h_m^s}{\in_{33}}\left(\frac{\partial^2 w}{\partial x^2} + \frac{\partial^2 w}{\partial y^2}\right) \tag{24}$$

in which $h_m^s = \left(\dfrac{h+h_s}{2}\right)$ and G is feedback gain.

3   GOVERNING EQUATIONS OF EQUILIBRIUM

The equation of motion for a FG rectangular plate with an actuator and a sensor patches bonded to the upper and lower faces, respectively and under distributive load of q, can be obtained using the classical plate theory and Navier equation. The motion equations are (see Fig. 1)

$$\sigma_{xx,x} + \sigma_{xy,y} + \sigma_{xz,z} = \rho\ddot{u}$$

$$\sigma_{yx,x} + \sigma_{yy,y} + \sigma_{yz,z} = \rho\ddot{v} \tag{25}$$

$$\sigma_{zx,x} + \sigma_{zy,y} + \sigma_{zz,z} = \rho\ddot{w}$$

Now, by integrating through the thickness of each laminate, the equilibrium equations can be obtained

$$
\begin{aligned}
N_{xx,x} + N_{xy,y} &= \bar{\rho}\ddot{u} \\
N_{yy,y} + N_{xy,x} &= \bar{\rho}\ddot{v} \\
M_{xx,xx} + 2M_{xy,xy} + M_{yy,yy} &= \bar{\rho}\ddot{w} - q
\end{aligned}
\tag{26}
$$

in which *q* represents the applied uniform distributed load over the plate surface. Collection of the equilibrium equations of actuator and sensor patch and rearranging them gives

$$
\begin{aligned}
N_{xx,x}^{a,s} + N_{xy,y}^{a,s} &= 0 \\
N_{yy,y}^{a,s} + N_{xy,x}^{a,s} &= 0 \\
M_{xx,xx}^{a,s} + 2M_{xy,xy}^{a,s} + M_{yy,yy}^{a,s} &= 0
\end{aligned}
\tag{27}
$$

and the equilibrium equations for FG plat (Host plat) are

$$
\begin{aligned}
N_{xx,x}^{H} + N_{xy,y}^{H} &= 0 \\
N_{yy,y}^{H} + N_{xy,x}^{H} &= 0 \\
M_{xx,xx}^{H} + 2M_{xy,xy}^{H} + M_{yy,yy}^{H} &= -(N_{xx}^{H}w_{,xx} + N_{yy}^{H}w_{,yy} + 2N_{xy}^{H}w_{,xy})
\end{aligned}
\tag{28}
$$

and the equilibrium equations for smart plat are

$$
\begin{aligned}
N_{xx,x} + N_{xy,y} &= 0 \\
N_{yy,y} + N_{xy,x} &= 0 \\
M_{xx,xx} + 2M_{xy,xy} + M_{yy,yy} &= -(N_{xx}^{H}w_{,xx} + N_{yy}^{H}w_{,yy} + 2N_{xy}^{H}w_{,xy})
\end{aligned}
\tag{29}
$$

Furthermore, the membrane resultant forces can be found as

$$
\begin{Bmatrix} N_{xx} \\ N_{yy} \\ N_{xy} \end{Bmatrix} = \int_{z_2}^{z_1} \begin{Bmatrix} \sigma_{xx}^{H} \\ \sigma_{yy}^{H} \\ \sigma_{xy}^{H} \end{Bmatrix} dz + \int_{z_1}^{z_0} \begin{Bmatrix} \sigma_{xx}^{a} \\ \sigma_{yy}^{a} \\ \sigma_{xy}^{a} \end{Bmatrix} R \ dz + \int_{z_3}^{z_2} \begin{Bmatrix} \sigma_{xx}^{s} \\ \sigma_{yy}^{s} \\ \sigma_{xy}^{s} \end{Bmatrix} R \ dz
\tag{30}
$$

and the resultant moments are

$$
\begin{Bmatrix} M_{xx} \\ M_{yy} \\ M_{xy} \end{Bmatrix} = \int_{z_2}^{z_1} \begin{Bmatrix} \sigma_{xx}^{H} \\ \sigma_{yy}^{H} \\ \sigma_{xy}^{H} \end{Bmatrix} z \ dz + \int_{z_1}^{z_0} \begin{Bmatrix} \sigma_{xx}^{a} \\ \sigma_{yy}^{a} \\ \sigma_{xy}^{a} \end{Bmatrix} R \ z \ dz + \int_{z_3}^{z_2} \begin{Bmatrix} \sigma_{xx}^{s} \\ \sigma_{yy}^{s} \\ \sigma_{xy}^{s} \end{Bmatrix} R \ z \ dz
\tag{31}
$$

Here σ_{ij}^{a}, σ_{ij}^{s} and σ_{ij}^{H} indicate the stress components of the, actuator, sensors and FG plate, respectively. *R* represents the location function (Box car function) defined as [26]

$$
R(x,y) = [H(x-La) - H(x+La)][H(y-Lb) - H(y+Lb)] = \begin{cases} 1 & -La < x < La, -Lb < y < Lb \\ 0 & \text{elsewhere} \end{cases}
\tag{32}
$$

in which, H is the Heaviside function. In addition, h_A, h_s and La and Lb are the thicknesses of the actuator and the sensor patches, the length and width of the sensor and actuator patches, respectively. Note that $I_0 = \int_{-h/2}^{h/2} \rho^H(z)\,dz$ is the mass density of FG plate and h represents the thickness of the FG plate and a and b are the length and the width of FG plate, respectively.

4　EQUILIBRIUM EQUATION OF SMART PLATE

By substituting Eqs. (4a), (4b) and (4c) into the stress-strain relation of the actuator, the sensor and FG plate i.e. Eqs. (8), (19) and (22) the stress components of the actuator, the sensor and the FG plate will be obtained. Then, by substituting the stress components of the smart plate into Eq. (31) the moment resultant equations as given as below

$$
\begin{bmatrix} M_{xx} \\ M_{yy} \\ M_{xy} \end{bmatrix} = \begin{bmatrix} c_1 & c_2 & c_3 \\ c_4 & c_5 & c_6 \\ c_7 & c_8 & c_9 \end{bmatrix} \begin{bmatrix} -\dfrac{\partial^2 w}{\partial x^2} \\ -\dfrac{\partial^2 w}{\partial y^2} \\ -\dfrac{\partial^2 w}{\partial x \partial y} \end{bmatrix}^a + \begin{bmatrix} b_1 & b_2 & b_3 \\ b_4 & b_5 & b_6 \\ b_7 & b_8 & b_9 \end{bmatrix} \begin{bmatrix} -\dfrac{\partial^2 w}{\partial x^2} \\ -\dfrac{\partial^2 w}{\partial y^2} \\ -\dfrac{\partial^2 w}{\partial x \partial y} \end{bmatrix}^s + \begin{bmatrix} k_1 & k_2 & k_3 \\ k_4 & k_5 & k_6 \\ k_7 & k_8 & k_9 \end{bmatrix} \begin{bmatrix} -\dfrac{\partial^2 w}{\partial x^2} \\ -\dfrac{\partial^2 w}{\partial y^2} \\ -\dfrac{\partial^2 w}{\partial x \partial y} \end{bmatrix}^H
$$

(33)

in which c_i, b_i and k_i components are

$$c_1 = c_{11}BR - \frac{e_{31}^2 G(h+h_S)h_S A}{2 \in_{33} h_A} R + \frac{e_{31}^2 R}{\in_{33}}\left(\frac{B}{3} - \frac{(h+h_A)A}{2}\right)$$

$$c_2 = c_{12}BR - \frac{e_{31}^2 G(h+h_S)h_S A}{2 \in_{33} h_A} R + \frac{e_{31}^2 R}{\in_{33}}\left(\frac{B}{3} - \frac{(h+h_A)A}{2}\right)$$

$$c_7 = c_8 = c_6 = c_3 = 0$$

$$c_4 = c_2$$

$$c_5 = c_1$$

$$c_9 = \frac{2c_{66}B}{3}R$$

$$b_1 = \frac{B_1 A_1}{3}R \qquad\qquad\qquad k_1 = \frac{D_1}{1-\upsilon^2}$$

$$b_2 = \frac{B_1 A_2}{3}R \qquad\qquad\qquad k_2 = \upsilon\frac{D_1}{1-\upsilon^2}$$

$$b_6 = b_7 = b_8 = b_3 = 0 \qquad\qquad k_3 = k_6 = k_7 = k_8 = 0$$

$$b_4 = b_2 \qquad\qquad\qquad\qquad k_4 = k_2$$

$$b_5 = b_1 \qquad\qquad\qquad\qquad k_5 = k_1$$

$$b_6 = \frac{2c_{66}B_1}{3}R \qquad\qquad\qquad k_9 = \frac{D_1}{1+\upsilon}$$

(34)

　　By substituting Eq. (33) into Eq. (29) and by further simplifications, the equilibrium equation of the smart plate is obtained and then for the rectangular FG plate with sensor and actuator patches, the general equilibrium equation reduces to the following

$$\left[\left(-\frac{1}{3}c_{11}B - \frac{Ae_{31}^2 Gh_S (h+h_S)}{2 \in_{33} h_A} + \frac{Ae_{31}^2 (h+h_A)}{2 \in_{33}} - \frac{e_{31}^2 B}{3 \in_{33}} - \frac{1}{3}\left(C_{11} + \frac{e_{31}^2}{\in_{33}}\right)B_1\right)R + \frac{D_1}{1-\upsilon^2}\right]\nabla^4 w = -N_x \frac{\partial^2 w}{\partial^2 x} \qquad (35)$$

where

$$\nabla^4 w = \frac{\partial^4 w}{\partial x^4} + 2\frac{\partial^4 w}{\partial x^2 \partial y^2} + \frac{\partial^4 w}{\partial y^4}, \qquad D_1 = \int_{-h/2}^{h/2} -z^2 E(z)\,dz \ , \qquad A_1 = \left(C_{11} - \frac{e_{31}^2}{\in_{33}}\right) \ , \quad A_2 = \left(C_{12} - \frac{e_{31}^2}{\in_{33}}\right) \qquad (36)$$

5 SOLUTION METHODOLOGY

To obtain the critical buckling load of the smart plate, the feedback gain is set to be zero. The Navier solution for the simply supported rectangular FG plate with actuator and sensor patches can be obtained by expanding the displacement in a Fourier series. Assume a double Fourier series for the lateral displacement as follows [24]

$$w = \sum\sum A_{mn} \sin\left(\frac{m\pi x}{a}\right)\sin\left(\frac{n\pi y}{b}\right) \qquad (37)$$

in which a and b are the length and width of FG plate. Substituting expression (37) into Eq. (35), the critical buckling load of the FG smart plate with piezoelectric patches, where the in-plane forces are $N_{xx} = -N_0$ can be obtained as

$$N_0(m,n) = \frac{\pi^2 a^2}{m^2}\left[\left\{\frac{1}{3}c_{11}B + \frac{Ae_{31}^2 Gh_S (h+h_S)}{2 \in_{33} h_A} - \frac{Ae_{31}^2 (h+h_A)}{2 \in_{33}} + \frac{e_{31}^2 B}{3 \in_{33}} + \frac{1}{3}(c_{11} + \frac{e_{31}^2}{\in_{33}})B_1\right\}R - \frac{D_1}{1-\upsilon^2}\right]\left(\frac{m^4}{a^4} + \frac{2m^2 n^2}{a^2 b^2} + \frac{n^4}{b^4}\right) \qquad (38)$$

and by further simplifications, it is obtained as

$$N_0(m,n) = \frac{\pi^2}{m^2 s^2 b^2}\left(FR - \frac{D_1}{1-\upsilon^2}\right)(m^4 s^4 + 2s^2 m^2 n^2 + n^4) \qquad (39)$$

where

$$s = \frac{b}{a} \ , \ D_1 = \int_{-h/2}^{h/2} -z^2 E(z)\,dz \ , \ F = \frac{1}{3}c_{11}B - \frac{Ae_{31}^2 Gh_S (h+h_S)}{2 \in_{33} h_A} - \frac{Ae_{31}^2 (h+h_A)}{2 \in_{33}} + \frac{e_{31}^2 B}{3 \in_{33}} + \frac{1}{3}(c_{11} + \frac{e_{31}^2}{\in_{33}})B_1 \qquad (40)$$

and R represents the location function (Boxcar function).

6 RESULTS AND DISCUSSION

In the present smart FG plate, a piezoelectric patch fixed to the bottom surface is considered to sense the strain and generates the electrical potential field and a piezoelectric patch fixed to the top surface, works as an actuator and controls the buckling of the structure. For this FG plate, the material and the geometrical properties are given in Table 1. The material and geometrical properties of piezoelectric patches for two types of PZT are given in Table 2. Further, it is assumed that $e_{ij}=e_{ji}$ for $i \neq j$. It should be noted that the first derivation of R, with respect to x or y yields to the delta function, i.e. $R_x = [\delta(x-La) + \delta(x+La)][H(y-Lb) + H(y+Lb)]$ and since, $\delta(y-Lb) = \delta(x-La) = 0$ then $R_x = R_y = R_{xx} = 0$.

Table 1
Material properties of the FG plate

FGM	$E(N/m^2)$	Total Thickness(m)	Size(m)
Aluminum oxide(ceramic)	3.202e11	1.6e-3	0.50×0.50
Ti-6A1-4V(metal)	1.057e11		

Table 2
Material properties of the piezoelectric patches (PZT) [26, 27]

Piezoceramic	C_{11}	C_{21}	d_{33}	d_{31}	d_{32}	e_{33}	e_{31}	e_{32}	$\in_{33}$	υ	Thickness (m)
PZT-4	1.38e11	77.8e10	289	-123	-123	15.08	-5.2	-5.2	1.15e-8	0.3	0.5e-3

To obtain the buckling load for an isotropic plate under uniaxial compressive force, values of β in the model of FGM and R in Eq. (39) should be equal to zero ($\beta = R = 0$). In this way, the piezoelectric and the FGM effects on the plate are ignored. By doing so, the buckling load can be obtained as follows

$$N_0(m,n) = \frac{\pi^2}{m^2 s^2 b^2}[\frac{D}{1-\upsilon^2}](m^4 s^4 + 2s^2 m^2 n^2 + n^4) \tag{41}$$

in which

$$D = \frac{Eh^3}{12(1-\upsilon^2)} \tag{42}$$

Eq. (41) in the non-dimensionalized form can be written as

$$\overline{N} = N_0 b^2 /(\pi^2 D) \tag{43}$$

After simplification and reduction of the model for isotropic plate, Eq. (41) agrees well with the result given in Ref. [20]. Fig. 2 shows the variation of non-dimensionalized buckling load for an isotropic plate vs. aspect ratio S (a/b). The trend of variation is again similar to the result obtained by Ref. [20]. In Fig. (3), the variation of the buckling load vs. feedback gain for different aspect ratio S is illustrated for PZT-4. By increasing S, the plate dimensions increases, which means that the plate tends to become more flexible and as it can be observed, the feedback gain is more dominant in increasing the critical buckling load. Fig. 4 shows the effect of feedback gain on buckling load of FG plate. It can be seen that for higher control gain, the buckling load of the plate is increased.
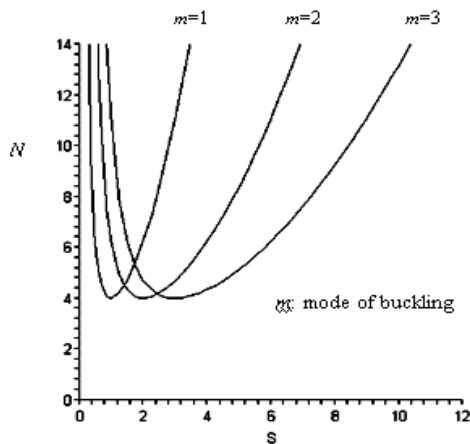

Fig. 2
Non-dimensionalized buckling load of an isotropic plate vs. S (a/b) for a simply supported plate (m=1, m=2, m=3), (β=0, R=0).
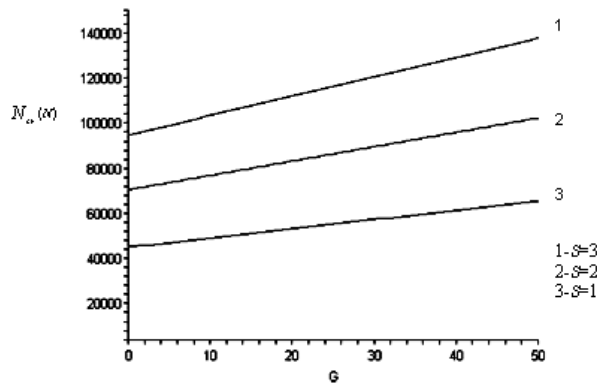
Fig. 3
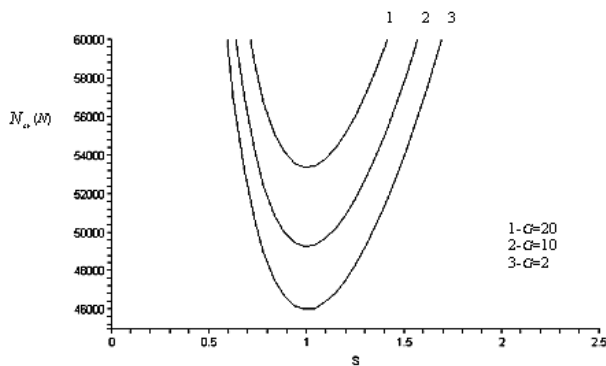Variation of buckling load vs. feedback gain for different values of S=a/b for PZT-4 (*R*=1).

Fig. 4
Variation of buckling load vs. S=a/b for different values of feedback control gain G and (*R*=1, PZT-4) (a) Gain=2, (b) Gain =10, (c) Gain=20.

7   CONCLUSION

In this paper, FG rectangular plate which is bonded with piezoelectric rectangular patch on the top and the bottom surface(s) as actuator/ sensor is considered. Under a constant electric charge, the governing differential equations of the motion for the plate are derived using classical laminated plate theory (CLPT). The solution for the motion equation is obtained using a Fourier series method and the effect of feedback gain and aspect ratio *S* on the critical buckling load is studied. Based on parametric study performed on this smart FG plate, it is concluded that:

1-The variation of critical buckling load vs. feedback gain indicates that by increasing the feedback gain, the buckling load increases.

2-By increasing *S*, the plate dimensions increases. It means that the plate is more flexible and the feedback gain is more dominant in increasing the critical buckling load.

REFERENCES

[1]   Brush D.O., Almroth B.O., 1975, *Buckling of Bars, Plates, and Shells*, McGraw-Hill, New York.
[2]   Turvey G., Marshall I., 1995, *Buckling and Postbuckling of Composite Plates*, Chapman-Hall, New York.
[3]   Eslami M.R., Shariyat M., 1997, Elastic, plastic and creep buckling of imperfect cylinders under mechanical and thermal loading, *ASME Transactions, Journal of Pressure Vessel Technology* **119** (1): 27-36.
[4]   Mossavarali A., Eslami M.R., 2002, Thermoelastic buckling of plates with imperfections based on higher order displacement field, *Journal of Thermal Stresses* **25**(8): 745-771.
[5]   Murphy K.D., Ferreira D., 2001, Thermal buckling of rectangular plates, *International Journal of Solids and Structures* **38** (22-23): 3979-3994.
[6]   Bailey T., Hubbard J.E., 1985, Distributed piezoelectric-polymer active vibration control of a cantilever beam, *Journal of Guidance, Control and Dynamics* **8**: 605-611.
[7]   Hauke T., Kouvatov A., Steinhausen R., Seifert W., Beige H., 2000, Bending behavior of functionally gradient materials, *Ferroelectrics* **238**: 759-766.

[8]   Fledman E., Aboudi J., 1997, Buckling analysis of functionally graded plates subjected to uniaxial loading, *Composite Structures* **38**: 29-36.

[9]   Woo J., Meguid S.A., 2001, Nonlinear analysis of functionally graded plates and shallow shells, *International Journal of Solids and Structures* **38**: 7409-7421.

[10] Javaheri R., Eslami M.R., 2002, Thermal buckling of functionally graded plates based on higher theory, *Journal of Thermal Stresses* **25**: 603-625.

[11] Tiersten HF., 1969, *Linear Piezoelectric Plate Vibrations*, Plenum, New York.

[12] Lee C.K., Moon F.C., 1989, Laminated piezopolymer plates for torsion and bending sensors and actuators, *Journal of the Acoustical Society of America* **85**: 2432-2439.

[13] Lee C.K., 1990, Theory of laminated piezoelectric plates for the design of distributed sensors/actuators-Part I: Governing equations and reciprocal relationships, *Journal of the Acoustical Society of America* **87**: 1144-1158.

[14] Thompson S.P., Loughlan J., 1995, The active buckling of some composite column strips using piezoceramic actuators, *Composite Structures* **32**: 59-67.

[15] Varelis D., Saravanos D., 2002, Nonlinear coupled mechanics and initial buckling of composite plate with piezoelectric actuators and sensors, *Smart Materials and Structures* **11**: 330-336.

[16] Yang J.S., 1999, Equations for thick elastic plates with partially electroded piezoelectric actuators and higher order electric fields, *Smart Materials and Structures* **8**: 73-82.

[17] Tzou H.S., 1993, Piezoelectric shells: Distributed sensing and control of continua, Dordrecht Kluwer Academic Publishers.

[18] Tzou H.S., Fu H.Q., 1994, Study of the segmentation of distributed piezoelectric sensors and actuators-Part I. Theoretical analysis, *Journal of Sound and Vibration* **172**(2): 247-259.

[19] Kargarnovin M.H., Najafizadeh M.M., Viliani N.S., 2007, Vibration control of a functionally graded material plate patched with piezoelectric actuators and sensors under a constant electric charge, *Smart Materials and Structures* **16**: 1252-1259.

[20] Reddy J.N., 1999, *Theory and Analysis of Elastic Plate*, Taylor and Francis Philadelphia, PA.

[21] Najafizadeh M.M., Eslami M.R., 2002, First-order theory based thermoelastic stability of functionally graded material circular plates, *AIAA Journal* **40**: 1444-1450.

[22] Ali O. Ayhan., 2007, Stress intensity factors for three-dimensional cracks in functionally graded materials using enriched finite element, *International Journal of Solids and Structures* **44**: 8579-8599.

[23] Lien W.C., Chung Y.L., Ching C.W, 2002, Dynamic stability analysis and control of a composite beam with piezoelectric layers, *Composite Structures* **56**: 97-109.

[24] Senthil V.G., 2001, Modeling of piezoelectric smart structures for active vibration and noise control application, PhD thesis, Department of Engineering Science and Mechanics, The University of Pennsylvania.

[25] Halliday D., Resnick R., Walker J., 2000, *Fundamentals of Physics*, Wiley, New York, Extended Sixth Edition.

[26] Wang D.A., Cheng C.H., Hsieh H.H., Zhang ZX., 2007, Analysis of an annular PZT actuator for a droplet ejector, *Sensor and Actuators A*: *Physical* **137**(2): 330-337.

[27] Zhang Q.M., Jianzhong Zhao., 1999, Electromechanical properties of lead zirconate titanatepiezocramic under the influence of mechanical stresses, *IEEE Transactions on Ultrasonics, Ferroelectrics and Frequency Control* **46**(6): 1518-1526.